Reduced model of a reaction-diffusion system for the collective motion of camphor boats

Kota Ikeda*
School of Interdisciplinary Mathematical Sciences, Meiji University, Tokyo 164-8525, Japan

Shin-Ichiro Ei
Department of Mathematics, Hokkaido University, Sapporo 060-0810, Japan

Masaharu Nagayama
Research Institute for Electronic Science, Hokkaido University, Sapporo 060-0811, Japan

Mamoru Okamoto
Graduate School of Science, Hokkaido University, Sapporo 060-0810, Japan

Akiyasu Tomoeda
Department of Mathematical Engineering, Musashino University, Tokyo 135-8181, Japan

(Received 23 November 2018; published 11 June 2019)

The unidirectional motion of a camphor boat along an annular water channel is observable. When camphor boats are placed in a water channel, both homogeneous and inhomogeneous states occur as collective motions, depending on the number of boats. The inhomogeneous state is a type of congestion, that is, the velocities of the boats change with temporal oscillation, and the shock wave appears along the line of travel of the boats. The unidirectional motion of a single camphor boat and the homogeneous state can be represented by traveling wave solutions in a mathematical model. Because the experimental results described here are thought of as a type of bifurcation phenomenon, the destabilization of traveling wave solutions may indicate the emergence of congestion. We previously attempted to study a linearized eigenvalue problem associated with a traveling wave solution. However, the problem is too difficult to analyze rigorously, even for just two camphor boats. Therefore we developed a center manifold theory and derived a reduced model in our previous work. In the present paper, we study the reduced model and show that the original model and our reduced model qualitatively exhibit the same properties by applying numerical techniques. Moreover, we demonstrate that the numerical results obtained in our models for camphor boats are quite similar to those in a car-following model, the *OV model*, but there are some different features between our reduced model and a typical OV model.

DOI: 10.1103/PhysRevE.99.062208

I. INTRODUCTION

Self-driven motion of animal and nonanimal organisms can be observed in several fields, such as biology [1], chemistry [2], and nonlinear physics [3,4]. Organisms move spontaneously to aggregate and form self-organized structures. In many cases, individual members do not interact directly. Rather, they change their surroundings in ways that have an influence on the behavior of other members, which implies that the organisms have long-range interactions [5,6]. Therefore it is important not only to clarify the mechanism of the self-sustaining motion of each organism, but also to study how organisms behave as a whole system.

Spatiotemporal collective motions in chemical experiments with camphor have been investigated experimentally and theoretically in Refs. [7–12]. A camphor scraping at an air-water surface exhibits several motions, including clockwise or counterclockwise rotation, and translation [9]. Furthermore, it was shown in Refs. [7,12,13] that unidirectional motion can be observed when we place a camphor boat in an annular water channel. In experimental setups, a camphor boat is composed of a plastic disk with a camphor disk stuck to its edge using an adhesive. Camphor boats constitute a system that exhibits two different states depending on the number of particles. It was reported in Ref. [12] that when the number of boats is less than 30, camphor boats move with a constant velocity and spatially disperse with the same spacing between boats. Such a homogeneous state is termed a *uniform flow* throughout this article. On the other hand, when the number is larger than 30, the velocities of the boats change with temporal oscillation, and a shock wave appears in the line of travel of the boats. We call such an inhomogeneous state generated by particles a *congested state*.

The spontaneous unidirectional motion of each camphor boat is realized as a traveling wave solution in the mathematical model proposed in Ref. [7] based on a Newtonian equation for the motion of a camphor boat and a reaction-diffusion

*ikeda@meiji.ac.jp

equation for the density of camphor molecules on the water surface. In the model, a traveling wave solution represents a state in which all camphor boats exhibit unidirectional motion with the same speed, and the same space exists between any pair of neighboring boats. Actually, such a model can also generate various collective motions of camphor boats. As seen in Figs. 3 and 4 of Ref. [12], congested states emerge in the model when the parameters and the number of boats are chosen appropriately. Therefore, it can be said that the numerical results qualitatively agree with those obtained through experiments.

The numerical results in Ref. [12] are also very similar to those in a car-following model, termed an *OV model* [14]. This is described by a form of ordinary differential equations, exhibiting a congested state of vehicles, and having a qualitative fit to the data widely extracted from highway traffic [15,16]. The authors of Ref. [12] state that the mathematical model for camphor boats can be reduced to an OV model under the assumption that the relaxation time and the decay length of camphor density on the water surface are much shorter than the motion of camphor boats and the boat length. Thus, because the reduced model is represented by a typical type of OV model, the mathematical model for camphor boats qualitatively may have the same mathematical structure as a typical OV model.

Here we recall that a traveling wave solution can emerge with a certain parameter set via pitchfork bifurcation in a model for camphor boats [7]. Generally speaking, a bifurcation point enables us to reduce a mathematical model to a lower dimensional dynamical system [17]. We follow a center manifold theory developed in Ref. [18] and have already derived a reduced system near a bifurcation point in our previous paper [19]. Another reduced system for a camphor boat has been derived in a formal manner, which verified that such a system can generate an oscillatory motion of the boat [20]. It was assumed in this previous work that the reduced system had high nonlinearity, despite there being no mathematical theories that guarantee the verification of the reduction process used to derive such nonlinearity. Thus, the aim in this study is to investigate our reduced system both mathematically and numerically. Moreover, we indicate the similarities and differences between the reduced system and a typical OV model.

This paper is organized as follows. In Sec. II we introduce a mathematical model, which is a modification of the model proposed in Ref. [7] [see (1)] and our reduced model [see (2)]. In Sec. III we provide several numerical results. First, space-time diagrams derived from (1) and (2) are shown, which indicate that the two models can generate congested states by changing the number of camphor boats. Second, typical *fundamental diagrams* are depicted, which are plots of the flow rate versus the number density of particles (boats). Finally, we apply a bifurcation analysis software called "AUTO" (see Ref. [21]) and demonstrate the global bifurcation structure of (2), in which we find a slight difference between (2) and a typical OV model. We note that it is difficult to apply AUTO to the original model (1) directly because (1) includes a form of a partial differential equation. In Sec. IV we formally discuss why our reduced model and the OV model can possess almost the same mathematical structure, discuss their differences, and then state our conclusions.

II. METHOD

A. Model for the self-sustaining motion of camphor boats

We introduce the following mathematical model for the self-sustaining motion of N camphor boats on the circuit $[0, L]$ [7,10,19]:

$$\begin{cases} \dfrac{d^2x_i}{dt^2}(t) = -\mu\dfrac{dx_i}{dt}(t) + F_i(t), \\ \dfrac{\partial u}{\partial t} = \dfrac{\partial^2 u}{\partial x^2} - ku + \displaystyle\sum_{i=1}^{N} f(x - x_i(t); s), \end{cases} \tag{1}$$

where k and μ are positive constants. In this model, a camphor boat is regarded as a particle, and the position of the ith camphor boat is denoted by $x_i(t)$ for $i = 1, \ldots, N$. The surface concentration of a camphor molecular layer is denoted by $u = u(x, t)$ at position x and time t. The first equation is described by the Newtonian equation with the surface tension determined by a nonlinear function γ of u. The difference in surface tension at the edge of the ith camphor boat is denoted by $F_i(t)$ and is defined by

$$F_i(t) = \frac{1}{2\rho}[\gamma(u(x_i(t) + \rho, t)) - \gamma(u(x_i(t) - \rho, t))],$$

where ρ is the radius of the camphor boats, and the nonlinear function $\gamma(u)$ is defined by $\gamma(u) = \gamma_1/(1 + au^n)$ for $a, \gamma_1, n > 0$ [7]. The surface concentration u of a camphor molecular layer is assumed to yield the reaction-diffusion equation with the function $f(x; s)$, defined by

$$f(x; s) = \begin{cases} 1, & 0 < x < \rho, \\ s, & -\rho < x < 0, \\ 0, & \text{otherwise}, \end{cases}$$

which means that camphor molecules are supplied only from $(-\rho, \rho)$ i.e., where a camphor boat contacts the water surface. Let $s \in [0, 1]$, which means that camphor boats may be inhomogeneous media and that the amount of the supply on $(-\rho, 0)$ is not larger than on $(0, \rho)$. The function u is assumed to satisfy the periodic boundary condition $x = 0, L$.

B. Reduced system

As seen in Fig. 1, (1) exhibits a congested state, which results from the destabilization of a uniform flow. In other words, the traveling wave solution of (1) must be unstable in a certain parameter region. Then we challenged this observation by studying the linearized eigenvalue problem of (1) to prove the instability of the uniform flow. However, it appears almost impossible to verify rigorously, even if there are only two boats. Thus we changed our approach to a reaction-diffusion type as in (1) and derived a more simplified model mathematically related to (1). The position and velocity of the ith particle are denoted by $x_i = x_i(t)$ and $v_i = v_i(t)$, respectively. Applying the theory in Ref. [22] to (1) in a formal manner, we can derive an ordinary differential system, which describes the

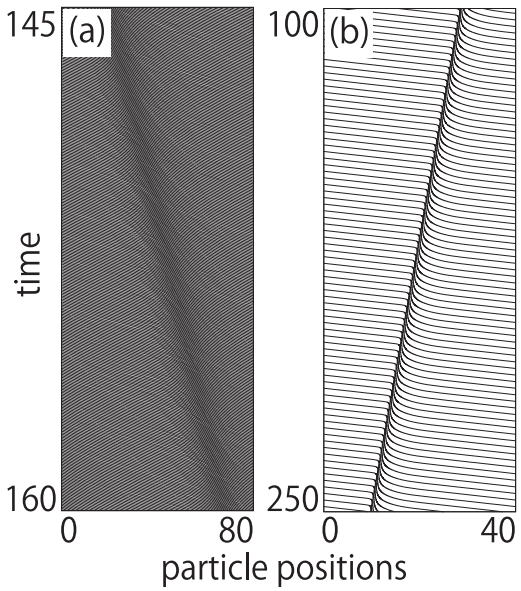

FIG. 1. Space-time diagrams for (1). Congested regions move forward (a) and backward (b). We set $N = 47, L = 80, \mu = 2, \rho = 0.25, k = 1.44, s = 0, \gamma_1 = 2112, a = 1, n = 2$, and the time increment is 0.00001 in panel (a), and $N = 8, L = 40, \mu = 5, \rho = 0.25, k = 5.5, s = 0, \gamma_1 = 20, a = 100$, and $n = 2$ in panel (b). In both panels, the number of the space grid is 2400.

dynamics of x_i and v_i, given by

$$\begin{cases} \dfrac{dx_i}{dt} = v_i, \\ \dfrac{dv_i}{dt} = G(v_i) + M_f e^{-\alpha(x_i - x_{i-1})} - M_b e^{-\beta(x_{i+1} - x_i)} \end{cases} \tag{2}$$

for $i = 1, \ldots, N$ and $G(v) = a_0 + a_1 v + a_2 v^2 + a_3 v^3$ for constants $a_0, a_1, a_2, a_3, M_f, M_b, \alpha$, and β. We assume that $0 \leqslant x_i(0) < x_{i+1}(0) < L$ for any $i = 1, \ldots, N-1$ and $x_i(t) \neq x_j(t)$ for $i \neq j$ and t. Because we suppose that $x_i(t)$ and $u(x,t)$ satisfy the periodic boundary conditions in (1), the position $x = L$ is identified with $x = 0$. In addition, we set $x_{N+1} = x_1 + L$ and $x_0 = x_N - L$. According to the center manifold theory, the bifurcation structure of (1) determines the nonlinear term $G(r)$, and a cubic function takes a canonical form in the case of pitchfork bifurcation [17]. Additionally, $M_f e^{-\alpha(x_i - x_{i-1})}$ and $M_b e^{-\beta(x_{i+1} - x_i)}$ represent the influence of the surface tension and of the diffusion of camphor molecules, respectively, from the neighboring particles. In the Supplemental Material [23], the process of the derivation of the reduced system is presented. The precise reduction process is also described in our pevious paper [19].

Mathematical analysis of (2) is much easier than that of (1) although we need more mathematical arguments to derive (2) from (1) rigorously (see Ref. [24]). More precisely, we assume that there exists a solution v for $G(v) + M_f e^{-\alpha L/N} - M_b e^{-\beta L/N} = 0$. Then the eigenvalue λ in the linearized eigenvalue problem of (2) associated with the uniform flow v can be explicitly represented by $\lambda = [G'(v) \pm \sqrt{G'(v)^2 - 4h(\omega)}]/2$, where $h(\omega) = \alpha M_f e^{-\alpha L/N}(1 - \omega) + \beta M_b e^{-\beta L/N}(1 - \overline{\omega}), \omega$ is a $(2N)$-th root of unity, and its complex conjugate is represented by $\overline{\omega}$. With this formula, we can easily study the parameter dependencies of λ and locate the bifurcation points. On the other hand, it is difficult to derive such an explicit characterization of eigenvalues for the uniform flow in (1). Therefore our reduced system (2) is useful for rigorous analysis.

C. Numerical simulations

We implement numerical simulations involving (1) and (2) for various densities of particles in a one-dimensional circuit. To change the density of particles continuously, we change the length L while maintaining the number of particles N as fixed. For the initial positions of particles, we consider only two cases. In the first case, we set $x_i(0) = iL/N$ for any i, which is called the *uniform* initial state. In the second case, we set $x_i(0) = iL/3N$ for any i, called the *congested* initial state. In other words, any two neighboring particles are positioned with the same distance in $(0, L)$ in the first case and in $(0, L/3)$ in the second case. Furthermore, we add small fluctuations for $x_i(0)$. The initial velocities of all particles are equal to 0. Integration of (2) was performed by applying the fourth-order Runge-Kutta iterative scheme with a time step of 0.0001.

We estimate the states of collective motions based on the flow rate of particles. Throughout this article, the flow rate is defined as the average of the velocities of all particles, which is more precisely given by

$$\frac{1}{L} \sum_{i=1}^{N} \frac{1}{T_2 - T_1} \int_{T_1}^{T_2} v_i(t)\, dt \tag{3}$$

for $T_1 < T_2$. This definition for the flow rate is slightly different from Ref. [12] but is analogous to that in traffic flow [25].

III. RESULTS

A. Space-time diagrams and fundamental diagrams

We first show that (1) can exhibit congested states as observed in the experiment in Fig. 3 of Ref. [12]. In Fig. 1 each solid line shows the position of each camphor boat at time t. A few camphor boats move at a relatively slower speed in a region which is relatively darker. We call such a region a *congested region*. Actually, the congested regions in Figs. 1(a) and 1(b) move forward and backward, respectively. As shown in Fig. 2(b) in Ref. [12], the congested region moves in the same direction as the motion of the camphor boats. However, the direction of motion of the congested region is opposite to that of the particles in the simulation (Fig. 3 in Ref. [12]).

We also obtain a fundamental diagram for (1). Figure 2 shows that the flow rate for low densities is monotonically increasing, while that for high densities is monotonically decreasing, which is qualitatively the same as the result of the experiment in Ref. [12]. To describe distinctive features of the fundamental diagram, we separate the density into five regions, as suggested in Ref. [15]. First, it is easy to verify the unique existence of a uniform flow in (1) for the parameter set of Fig. 2. In Region I, only uniform flow emerges, and the flow rates increase monotonically in both initial states. In Region III, the uniform flow is destabilized and a stable congested state is achieved. These results indicate that the uniform flow becomes unstable as the density increases. Although the

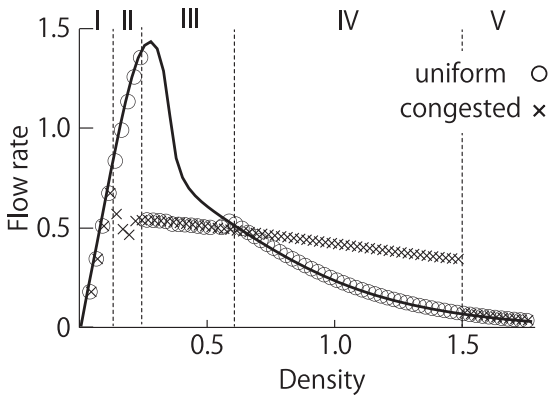

FIG. 2. Fundamental diagram in (1). The circles and crosses denote the flow rates for the solutions having a uniform initial state and a congested initial state, respectively. All velocities of particles are assumed to be 0 initially, and all parameters are the same as in Fig. 1(b) except for L. We set $T_1 = 100$ and $T_2 = 400$ in (3) to compute the flow rates.

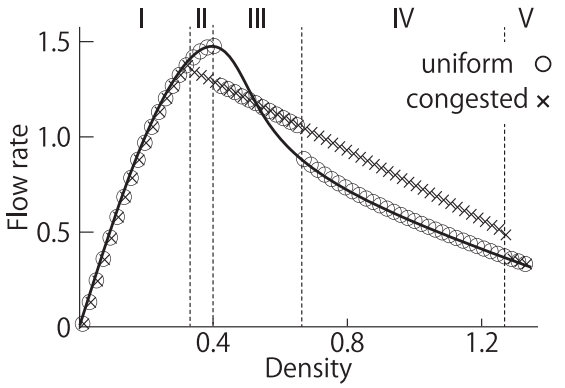

FIG. 4. Fundamental diagram in (2). The circles and crosses denote the flow rates for the solutions having a uniform initial state and a congested initial state, respectively. All velocities of particles are assumed to be 0 initially. In both cases, $N = 40, M_f = 0, M_b = 31.6875, \alpha = 0.0, \beta = 0.42$, $a_0 = 25.35, a_1 = -9.49, a_2 = 2.78$, and $a_3 = -0.338462$. We set $T_1 = 500$ and $T_2 = 1000$ in (3) to compute the flow rates.

uniform flow cannot be realized in Region III, it reappears in Regions IV and V. On the other hand, a congested state can be observed not only in Region III, but also in Regions II and IV. Therefore, the uniform flow and the congested state can coexist in Regions II and IV. Note that these results are completely consistent with those in Ref. [15].

Next we show numerical results generated by our reduced model given by (2). We find in Fig. 3 that both a uniform flow and a congested state appear from (2) depending on the density of particles. As well as Fig. 1, each solid line represents the position of each particle at time t. Note that all parameters are the same except for the length of the circuit L in Figs. 3(a) and 3(b). The difference between the densities of particles in Figs. 3(a) and 3(b) results in destabilization of the uniform flow, as seen in Fig. 3(a), and emergence of the congested state in Fig. 3(b). In Figs. 3(b) and 3(c), different types of congested states appear. There is one congested region in each figure, Figs. 3(b) and 3(c). The directions of the congested region in Figs. 3(b) and 3(c) are antiparallel and parallel to the motions of the particles, respectively. These results are also obtained using (1). Moreover, the fundamental diagram shown in Fig. 4 for (2) is qualitatively the same as in Fig. 2. Our system given by (2) as well as (1) can yield the same results as observed in the experiments by selecting the system parameters appropriately.

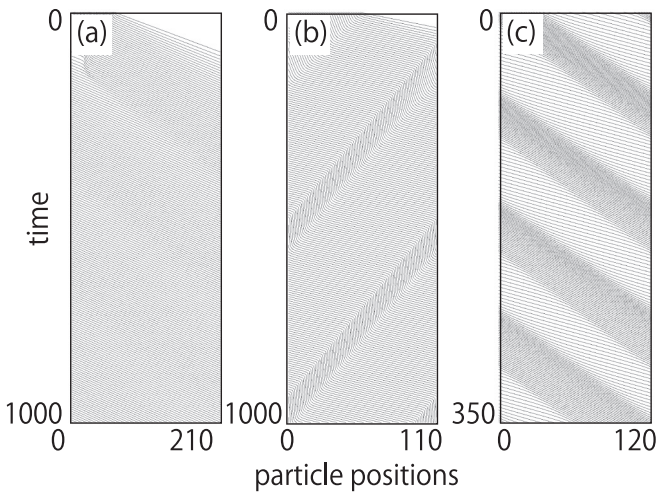

FIG. 3. Space-time diagrams for (2) [(a) uniform flow; (b, c) congested states]. In panels (a) and (b), all parameters are the same except for the length of the circuit L. We set $L = 210$ in panel (a) and $L = 110$ in panel (b), respectively. Only the difference between the densities of particles in panels (a) and (b) causes the uniform flow shown in panel (a) to no longer be stable in panel (b). In panels (b) and (c), different types of congested states emerge, and the congested region moves backward in panel (b) and forward in panel (c). We set $N = 31, M_f = 0, M_b = 1.5, \beta = 0.21, a_0 = 1.2, a_1 = -1.46, a_2 = 1.39$, and $a_3 = -0.55$ in panels (a) and (b), and $N = 31, L = 120, M_f = 0, M_b = 2.6, \beta = 0.1, a_0 = 8.0, a_1 = -5.2, a_2 = 1.42$, and $a_3 = -0.14$ in panel (c).

B. Global bifurcation diagram in (2) and multiple congested regions

Applying the AUTO software to (2), we can present a global bifurcation diagram (see Fig. 5). The figure consists of a straight line and six curves, which correspond to the uniform flow and to periodic solutions of (2), respectively. The three curves D, E, and F are dashed, which implies that all periodic solutions on those branches are unstable. On the other hand, curves A, B, and C include both solid and dashed marks. This means that stable periodic solutions emerge via bifurcation. In particular, we find a stable congested state at each point on the solid curve of A, which is consistent with the results for a typical OV model obtained in Ref. [26], meaning that a congested state has only one congested region. On the other hand, stable periodic solutions with multiple congested regions can be observed on the solid curves in B and C. Moreover, such stable periodic solutions can coexist. For example, setting $L = 50$ and carrying out numerical simulations of (2), we obtain three types of periodic solutions with different numbers of congested regions. In Figs. 6(a)–6(c) there are one, two, and three congested regions in the circuit, respectively. Because

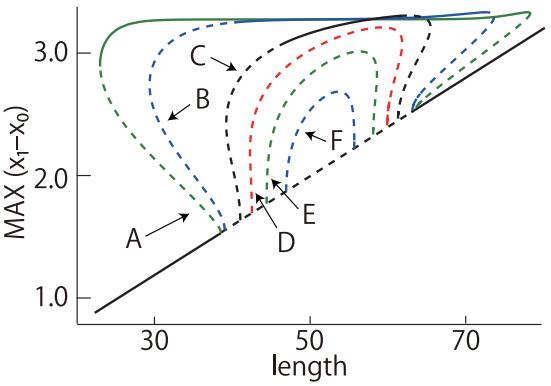

FIG. 5. Bifurcation diagram using (2). This numerical analysis was performed with AUTO. The solid and dashed lines show that associated solutions are stable or unstable, respectively. We set $N = 25$. The other parameters in (2) are the same as those in Fig. 4.

we fix $L = 50$ and all the parameters in the simulations are the same as those used in Fig. 5, only the differences in the initial conditions affect the numerical results. Such solutions with multiple congested regions cannot be observed in the OV model, as stated in Ref. [14]. Therefore, we conclude that our reduced model (2) has many of the same features as a typical OV model but exhibits a qualitatively different mathematical structure.

We discuss the qualitative properties of congested regions, which are symbolized by R_i $(i = 1, \ldots, 6)$ in Figs. 6(a)–6(c) more precisely. Each congested region moves backward with respect to the moving direction of particles with a constant velocity, and the cluster size, which is referred to as the number of particles in the region and was introduced in Ref. [14], is constant in time. All congested regions have almost the same velocities, which are estimated as 0.918 (R_1), 0.916 (R_2), 0.91 (R_3), and 0.89 (R_4, R_5, and R_6). It appears that any neighboring congested regions among R_4, R_5, and R_6 have similar separation in Fig. 6(c), but the separation of two intervals between congested regions R_2 and R_3 is different.

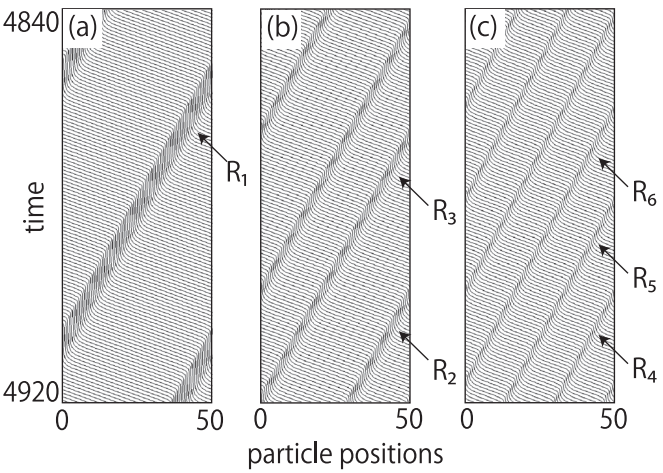

FIG. 6. Space-time diagrams for (2). We set $L = 50$ and $N = 25$ and applied the same parameters used in Fig. 4 for all numerical results (a)–(c). On the other hand, the initial conditions are different.

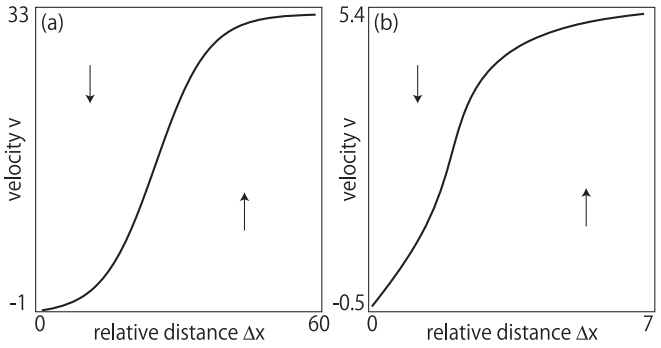

FIG. 7. Dynamics of (4) and (5) for each Δx. The solid lines are graphs of $v = V(\Delta x)$ in panel (a) and $v = G^{-1}(M_b e^{-\beta \Delta x})$ in panel (b), where G^{-1} is the inverse function of G. To show the results in panel (a), we set $V(\Delta x) = a[\tanh \beta(\Delta x - \Delta x_0) + M]$ with $a = 16.8$, $\beta = 0.086$, $\Delta x_0 = 25$, $M = 0.913$, which are the same parameters as in Ref. [15], while all parameters used for panel (b) are the same as in Fig. 4.

IV. SUMMARY AND DISCUSSION

In the present article, congested states of camphor boats, which are types of collective motions in a one-dimensional lane, have been studied using theoretical approaches. The experimental results shown in Fig. 2 of Ref. [12] indicate that camphor boats exhibit both a uniform flow and a congested state depending on the density of particles. Such qualitative behaviors of camphor boat motions are consistent with those of traffic flow described in Ref. [14]. From this viewpoint, we have investigated the mathematical model given by (1) and the reduced system given by (2) theoretically and numerically to clarify the similarities and differences between these models and a typical OV model.

The space-time diagrams for (1) and (2) are qualitatively the same as for a typical OV model (see Figs. 1 and 3). The fundamental diagrams in Figs. 2 and 4 are very similar to that in Ref. [15]. These facts imply that (1), (2), and the OV model share the same mathematical structure for exhibiting congestion phenomena, although they also differ in some behaviors, as discussed below.

To highlight the similarities based on the qualitative properties of (2) and the OV model, we focus on the following two equations:

$$\frac{dv}{dt} = a[V(\Delta x) - v], \tag{4}$$

$$\frac{dv}{dt} = G(v) - M_b e^{-\beta \Delta x}, \tag{5}$$

where $V(\Delta x)$ in (4) is smooth, uniformly bounded, and monotonically increasing, called an *optimal velocity function* or *OV function*. Equations (4) and (5) are associated with the OV model and (2), respectively. These are ordinary differential equations for velocity v with relative distance Δx. Here we consider Δx as a fixed parameter. Figure 7 shows the dynamics of the solutions and the graphs of the nullclines of (4) and (5). Moreover, the arrows in the figures are associated with the vector fields of (4) and (5) for each $\Delta x > 0$, which implies that velocity v in each equation converges to a steady state for

any initial value and Δx. The Δx dependency of the nullcline shown in Fig. 7(a) is qualitatively the same as in Fig. 7(b) based on the facts that it increases monotonically, converges in the limit $\Delta x \to \infty$, and has only one inflection point. We expect that these similarities qualitatively generate the same behaviors in the solutions obtained by the OV model and (2).

We have found some differences between the models for camphor boats and a typical OV model. The first is the flow direction of a congested region. In the traffic flow model, the congested region moves in a direction opposite to the motion of each particle. On the other hand, the congested region of camphor boats moves in the same direction as the motion of each particle in the experiment. By selecting system parameters appropriately, (1) and (2) can also exhibit both congested states with congested regions whose directions are parallel and antiparallel to the motions of particles. As far as we know, no previous research has worked out a simulation for a reaction-diffusion model such as that represented by (1), in which the same results as in the experiment are generated. To conclude, the system defined by (2) not only is written in the form of simple ordinary differential equations, but also has a rich structure.

Second, we noted a difference in the global bifurcation diagrams numerically obtained with AUTO. As stated in Ref. [26], any state with multiple congested regions appears to be unstable and gradually transitions to a state with a single congested region in the OV model. On the other hand, (2) exhibits stable congested states, which can involve multiple congested regions. Moreover, such states can coexist using the same parameter set. In conclusion, we can state the possibility that the collective motions observed in camphor boats include qualitatively different properties from those in vehicles.

ACKNOWLEDGMENTS

This work was supported by JSPS KAKENHI Grant No. JP15K17594 to K.I., JST CREST Grant No. JPMJCR15D2 and JSPS KAKENHI Grant No. JP16H03949 to M.N., JST CREST Grant No. JPMJCR14D3 to S.E., and JSPS KAKENHI Grant No. JP17K05147 to A.T., Japan. The authors would like to express their appreciation to the referees for their useful suggestions and comments which have improved the original manuscript. Moreover, the authors would like to thank Nobuhiko J. Suematsu (Meiji University, Japan) and Kei Nishi (Kyoto Sangyo University, Japan) for their stimulating discussions, and Editage (www.editage.jp) for English language editing.

[1] T. Miura and R. Tanaka, In vitro vasculogenesis models revisited-measurement of VEGF diffusion in matrigel, Math. Model. Natural Phenom. **4**, 118 (2009).

[2] M. K. Chaudhury and G. M. Whitesides, How to make water run uphill, Science **256**, 1539 (1992).

[3] D. Helbing, I. Farkas, and T. Vicsek, Simulating dynamical features of escape panic, Nature (London) **407**, 487 (2000).

[4] A. Tomoeda, K. Nishinari. D. Chowdhury and A. Schadschneider, An information-based traffic control in a public conveyance system: Reduced clustering and enhanced efficiency, Physica A **384**, 600 (2007).

[5] E. Heisler, N. J. Suematsu, A. Awazu, and H. Nishimori, Swarming of self-propelled camphor boats, Phys. Rev. E **85**, 055201(R) (2012).

[6] M. Inaba, H. Yamanaka, and S. Kondo, Pigment pattern formation by contact-dependent depolarization, Science **335**, 677 (2012).

[7] M. Nagayama, S. Nakata, Y. Doi, and Y. Hayashima, A theoretical and experimental study on the unidirectional motion of a camphor disk, Physica D **194**, 151 (2004).

[8] X. Chen, S.-I. Ei, and M. Mimura, Self-motion of camphor discs: Model and analysis, Netw. Heterogen. Media **4**, 1 (2009).

[9] S. Nakata, Y. Iguchi, S. Ose, M. Kuboyama, T. Ishii, and K. Yoshikawa, Self-rotation of a camphor scraping on water: New insight into the old problem, Langmuir **13**, 4454 (1997).

[10] S. Nakata, M. Nagayama, H. Kitahata, N. J. Suematsu, and T. Hasegawa, Physicochemical design and analysis of self-propelled objects that are characteristically sensitive to environments, Phys. Chem. Chem. Phys. **17**, 10326 (2015).

[11] K. Nishi Kei, K. Wakai, T. Ueda, M. Yoshii, Y. S. Ikura, H. Nishimori, S. Nakata, and M. Nagayama, Bifurcation phenomena of two self-propelled camphor disks on an annular field depending on system length, Phys. Rev. E **92**, 022910 (2015).

[12] N. J. Suematsu, S. Nakata, A. Awazu, and H. Nishimori, Collective behavior of inanimate boats, Phys. Rev. E **81**, 056210 (2010).

[13] S. Nakata, M. Kohira, and Y. Hayashima, Mode selection of a camphor boat in a dual-circle canal, Chem. Phys. Lett. **322**, 419 (2000).

[14] M. Bando, K. Hasebe, A. Nakayama, A. Shibata, and Y. Sugiyama, Structure stability of congestion in traffic dynamics, Jpn. J. Ind. Appl. Math. **11**, 203 (1994).

[15] M. Bando, K. Hasebe, K. Nakanishi, A. Nakayama, A. Shibata, and Y. Sugiyama, Phenomenological study of dynamical model of traffic flow, J. Phys. I **5**, 1389 (1995).

[16] Y. Sugiyama, M. Fukui, M. Kikuchi, K. Hasebe, A. Nakayama, K. Nishinari, S.-I. Tadaki, and S. Yukawa, Traffic jams without bottlenecks: Experimental evidence for the physical mechanism of the formation of a jam, New J. Phys. **10**, 033001 (2008).

[17] Y. A. Kuznetsov, *Elements of Applied Bifurcation Theory*, 3rd ed., Applied Mathematical Sciences Vol. 112 (Springer-Verlag, New York, 2004).

[18] S.-I. Ei, The motion of weakly interacting pulses in reaction-diffusion systems, J. Dyn. Diff. Eq. **14**, 85 (2002).

[19] S.-I. Ei, K. Ikeda, M. Nagayama, and A. Tomoeda, Reduced model from a reaction-diffusion system of collective motion of camphor boats, Discrete Contin. Dyn. Syst. Ser. S **8**, 847 (2015).

[20] Y. Koyano, T. Sakurai, and H. Kitahata, Oscillatory motion of a camphor grain in a one-dimensional finite region, Phys. Rev. E **94**, 042215 (2016).

[21] E. J. Doedel and B. E. Oldeman, AUTO-07P: Continuation and bifurcation software for ordinary differential equations (Concordia University, Montreal, Canada, 2012).

[22] S.-I. Ei, M. Mimura, and M. Nagayama, Pulse–pulse interaction in reaction–diffusion systems, Physica D **165**, 176 (2002).

[23] See Supplemental Material at http://link.aps.org/supplemental/10.1103/PhysRevE.99.062208 for a detailed derivation of the reduced system.

[24] S.-I. Ei and K. Ikeda, Reductive approach for collective motions of camphor boats with delta functions (unpublished).

[25] D. Helbing, Traffic and related self-driven many-particle systems, Rev. Mod. Phys. **73**, 1067 (2001).

[26] I. Gasser, G. Sirito, and B. Werner, Bifurcation analysis of a class of 'car following' traffic models, Physica D **197**, 222 (2004).